Differences in coastal and oceanic SST trends north of Yucatan Peninsula

R. Varela, X. Costoya, C. Enriquez, F. Santos, M. Gómez-Gesteira

PII: S0924-7963(17)30331-7
DOI: doi:10.1016/j.jmarsys.2018.03.006
Reference: MARSYS 3065

To appear in: *Journal of Marine Systems*

Received date: 28 July 2017
Revised date: 15 February 2018
Accepted date: 20 March 2018

Please cite this article as: R. Varela, X. Costoya, C. Enriquez, F. Santos, M. Gómez-Gesteira , Differences in coastal and oceanic SST trends north of Yucatan Peninsula. The address for the corresponding author was captured as affiliation for all authors. Please check if appropriate. Marsys(2017), doi:10.1016/j.jmarsys.2018.03.006

Differences in coastal and oceanic SST trends north of Yucatan Peninsula

*** R. Varela[1], X. Costoya[2], C. Enriquez[3],** F. Santos[1,2], M. Gómez-Gesteira[1]

1 Ephyslab, Environmental Physics Laboratory, Facultad de Ciencias, Universidad de Vigo, 32004 Ourense, Spain, ruvarela@uvigo.es.

2 CESAM, Departamento de Física, Universidade de Aveiro, 3810-193 Aveiro, Portugal.

3 Facultad de Ciencias, Universidad Nacional Autónoma de México, Sisal Yucatán, México.

Abstract

The coastal area north of Yucatan has experienced a cooling SST trend from 1982 to 2015 during the upwelling season (May-September) that contrasts with the warming observed at the adjacent ocean area. Different drivers were analyzed to identify the possible causes of that unusual coastal cooling. Changes in coastal upwelling and in sea-atmosphere heat fluxes are not consistent with the observed coastal cooling. The eastward shift of the Yucatan Current observed over the last decades is hypothesized as the most probable cause of coastal cooling. This shift enhances the vertical transport of cold deeper water to the continental shelf from where it is pumped to the surface by upwelling favorable westerly winds.

Keywords: Upwelling, Yucatan, sea surface temperature, wind, current direction, shelf dynamics, warming, cooling

1. Introduction

Over the last decades, the scientific community has focused its attention on the impact of climate change. Ocean plays a key role in regulating that impact since it has absorbed the vast majority of the heat gained by the Earth (Levitus et al., 2005, Mikaloff-Fletcher et al., 2006, Levitus et al., 2012).

Upwelling systems are productive oceanic areas with important socio-economic implications. In fact, upwelling systems only occupy 1% of the world's ocean but more than 20% of fish catches occurs there (Pauly and Christensen, 1995). These systems are especially vulnerable to climate change that can affect not only the physical component (water temperature and wind patterns) but also productivity of the area.

Regarding ocean temperature, several authors have observed different rates of warming depending on the location (Harrison and Carson, 2007; Lima and Wethey, 2012, Cheung et al., 2013). This variability is even more marked at regional scale. In this way, a different warming rate has been observed for coastal and oceanic locations in some of the most important upwelling systems: Benguela, Canary, West Iberian Peninsula, Java or La Guajira (Lemos and Sansó, 2006, Santos et al., 2012a,b,c, Santos et al., 2016, Varela et al., 2016). Most of these studies have linked the different warming rates at coast and ocean with the strengthening of coastal upwelling, which can act as a moderator of climate change. A complete study about the evolution of upwelling in the main upwelling areas worldwide can be observed in Varela et al., (2015).

In the coastal zone of the Yucatan Peninsula two very different upwelling processes occur: a typical wind related upwelling in the northern coast of the Peninsula and a dynamic upwelling in the northeastern corner of the Peninsula. Yucatan is localized in the south-eastern area of the Gulf of Mexico around 21ºN and between 269-274ºE (Figure 1). The northern coast of the Yucatan Peninsula follows a marked zonal

orientation. In general, the area is characterized by a wide continental shelf that extends over 250 km (Ruiz-Castillo et al., 2016), being much narrower east of the Yucatan Peninsula. Easterly and northeasterly winds (trade winds) prevail throughout the year giving rise to conditions that favor upwelling over the northern coast of the Yucatan shelf (Merino, 1997, Pérez-Santos et al., 2010, Enríquez et al., 2013, Ruiz-Castillo et al., 2016). Ruiz-Castillo et al., (2016) examined coastal upwelling using Advanced Very High Resolution Radiometer (AVHRR) and Cross-Calibrated Multi-Platform (CCMP) from 1986 to 2009 and 1988 to 2011, respectively, to analyze SST and wind patterns. These authors obtained positive values of upwelling index (UI) throughout the year, with the highest values observed from March to July. Similar results were obtained by Pérez-Santos et al., (2010), who considered that Ekman Transport was the main process favoring permanent coastal upwelling at the northern coast of the Yucatan Peninsula. The prevalence of upwelling favorable winds confers this region distinguishable chlorophyll-a properties when compared with adjacent areas, highlighting the biological impact of upwelling (Salmerón-García et al., 2011, Pérez-Santos et al., 2014).

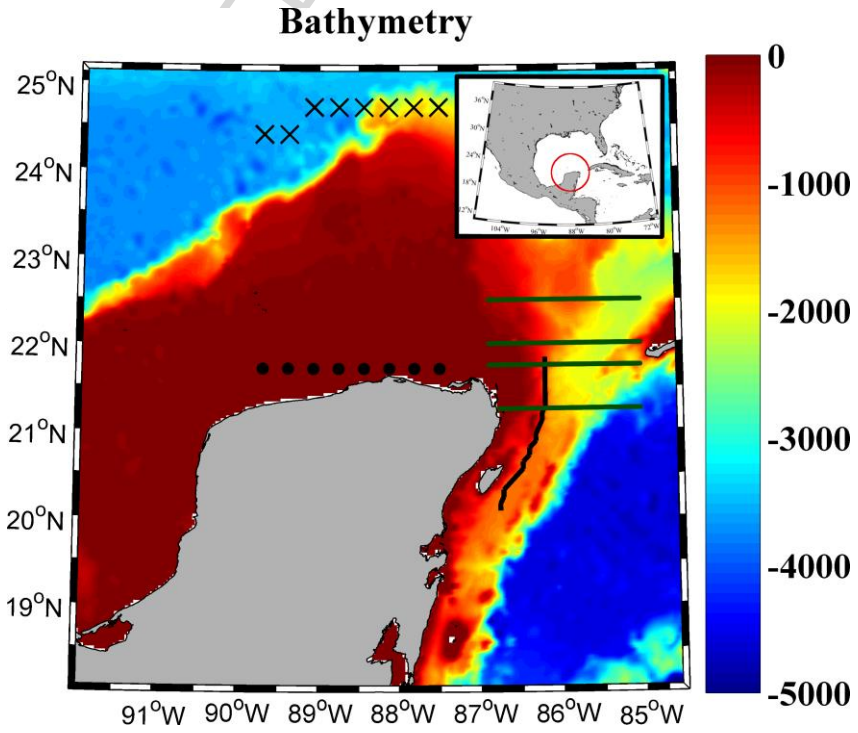

Figure 1 | Bathymetry of the area under study. Dots (crosses) mark the coastal (oceanic) location where wind and SST were obtained. The solid black line represents the transect where temperature variability was analyzed along the Yucatan current. The solid green lines represent the transects where subsurface water that upwells to the Yucatan shelf was analyzed.

A different upwelling process occurs form April to September in the form of sharp and intense pulses of deeper water masses into the northeastern corner of Yucatan, attracting species of ecological and commercial interest as the whale shark (*Rhincodon typus*) (Cárdenas-Palomo et al., 2015). Actually, the upwelling region has been declared a biosphere reserve for this specie. It is crucial to analyze temperature variation in this area, especially within the context of climate change, since changes in warming patterns can induce changes in biodiversity at the ecosystem level (e.g: latitudinal shifts on the distribution of species).

Different authors have focused their research on SST patterns in this area. A cold band is observed during summer months along the coast associated with upwelling favorable winds (Zavala-Hidalgo et al., 2006, Ruiz-Castillo et al., 2016). A 7 years analysis of SST from AVHRR satellite carried out by Zavala-Hidalgo et al., (2006) showed cold coastal water in Yucatan from May to August with a peak in July, during these months the difference in temperature between coast and ocean can be up to 2ºC. del Monte-Luna et al., (2015) related the recurrent upwelling in the area to the cold water found north of Yucatan Peninsula. Ruiz-Castillo et al., (2016) observed a cold water band in the inner shelf starting in April with differences up to 1ºC with the warm waters off the Yucatan shelf. This effect continues at least until October. Regarding SST trends, Lima and Wethey, (2012) used data from AVHRR to analyze SST variations over the period

1982-2010. For the case of Yucatan, they obtained a slight cooling during most of the year. However, that cooling trend cannot be associated with positive trends of UI in the area as observed in other regions (Santos et al., 2012a,b,c). In fact, Varela et al., (2015) obtained negative trends of wind stress for the area of Yucatan using wind stress data from the Climate Forecast System Reanalysis (CFSR) over the same period.

Other authors have pointed out that wind forcing is not enough to explain the appearance of colder water in the innermost area of the Yucatan shelf (Enríquez and Mariño-Tapia, 2014; Reyes-Mendoza et al., 2016; Souza et al., 2016; Carrillo et al., 2016). Enríquez and Mariño-Tapia, (2014) found that the characteristics of the Yucatan Current (YC) could influence the upwelling in the area, in such a way that, when YC separates from the continental slope, favors the enhancement of positive vertical velocities, which raise cold, nutrient rich water to the surface layer. Similar results were obtained by Carrillo et al., (2016) who observed an uplifting of the isotherms under the action of the YC, which evidence the existence of upwelling in the area. Thus, the enhancement of the YC can lead to the reinforcement of upwelling in the area (Enríquez and Mariño-Tapia, 2014; Carrillo et al., 2016, Souza et al., 2016).

The aim of this paper is to analyze SST variability along the Yucatan upwelling system over the last three decades. This variability will be related to different drivers like upwelling index, heat exchange with the atmosphere or changes in the Yucatan current. As far as we know, this is the first long term study on SST variability in the area. Previous works analyzed upwelling and SST pattern (Zavala-Hidalgo et al., 2006, Ruiz-Castillo et al., 2016), but they were not focused on long term SST changes within a framework of global warming. In addition, the present work also relates the observed SST changes to the different drivers that affect water temperature in the zone.

2. Data and Methods

2.1. Temperature data

Daily SST values were retrieved from the Optimum Interpolation Sea Surface Temperature (OISST) ¼ database (https://www.ncdc.noaa.gov/oisst). This database was built by means of Advanced Very High Resolution radiometer (AVHRR) infrared satellite SST data and data from ships and buoys (Reynolds, 2009 and Reynolds and Chelton, 2010). A special method of kriging (Optimum interpolation) was used to construct a regular grid (0.25º × 0.25º) containing data from 1982 to 2015.

Sea Temperature data along the water column was obtained from the Hybrid Coordinate Ocean Model (HYCOM). HYCOM uses satellite altimeter observations, satellite and in-situ sea surface temperature. Also, in-situ vertical temperature and salinity profiles from XBTs, ARGO floats, and moored buoys, using the NRL-developed Navy Coupled Ocean Data Assimilation (NCODA) system (Cummings, 2005; Cummings and Smedstad, 2013). HYCOM has a horizontal resolution of 1/12º×1/12º at 3-hour time steps and 40 standard depth levels covering the period from 1993 to present.

2.2. Wind data

Wind data were obtained from the NCEP CFSR database at http://rda.ucar.edu/pub/cfsr.html developed by the National Oceanic and Atmospheric Administration (NOAA). Data were acquired from the NOAA National Operational Model Archive and Distribution System, which is supported by the NOAA National Climatic Data Center (Saha et al., 2010). Wind was calculated at a reference height of 10 m with 6-hourly time resolution. The spatial resolution was 0.3º×0.3º from January 1982 to April 2011 and 0.2º×0.2º from then on. A common resolution over the whole period under study was used by interpolating data on a 0.3º×0.3º grid. Daily wind data

were averaged at monthly scale. Only coastal pixels with less than 25% of land were used to avoid problems with land contamination.

Ekman Transport components were calculated following:

$$Q_x = \frac{\rho_a C_d}{\rho_w f} (W_x^2 + W_y^2)^{\frac{1}{2}} W_y \quad (1)$$

$$Q_y = -\frac{\rho_a C_d}{\rho_w f} (W_x^2 + W_y^2)^{\frac{1}{2}} W_x \quad (2)$$

where Q_x and Q_y are the zonal and meridional components of the Ekman Transport, W_x and W_y are the zonal and meridional components of wind, $\rho_w = 1025 Kgm^{-3}$ is the sea water density, $C_d = 1.4 \times 10^{-3}$ the drag coefficient, $\rho_a = 1.22 Kgm^{-3}$ the air density and f is the Coriolis parameter defined as $f = 2\Omega \sin(\theta)$ where Ω is the angular velocity and θ the latitude.

UI is the Ekman transport component in the direction perpendicular to the shoreline (Nykjaer and Van Camp, 1994):

$$UI = -\sin\left(\Psi - \frac{\pi}{2}\right) Q_x + \cos\left(\Psi - \frac{\pi}{2}\right) Q_y \quad (3)$$

where Ψ is the angle of the unitary vector perpendicular to the coastline pointing oceanward. In this study the angle was set to 90º for the whole region. Positive (negative) upwelling indices correspond to upwelling-favorable (unfavorable) conditions.

2.3. Ocean currents

The velocity components (zonal and meridional) were also obtained from the HYCOM + NCODA Global 1/12° Reanalysis database (see description above). Each velocity component is characterized by three indices (i, j, k) that determine the grid point.

2.4. Heat flux data

Heat fluxes were also obtained from CFSR database (see description above). Shortwave, longwave, latent heat and sensible heat were retrieved at monthly scale from

1982 to 2015. Total net heat flux (Q_T) through the ocean surface was calculated following equation (4):

$$Q_T = Q_{SW} + Q_{LW} + Q_S + Q_L \quad (4)$$

Where Q_{SW} is the shortwave flux, Q_{LW} is the longwave flux, Q_S is the sensible heat flux and Q_L is the latent heat flux. Negative (positive) heat fluxes imply that ocean is losing (gaining) heat.

2.5. Calculation of trends

Trends were calculated at each pixel as the slope of the linear regression of the anomaly of each variable versus time. Monthly anomalies at a given month were calculated by subtracting from the monthly value the mean value of that month over the period 1982-2015. Trends were calculated using raw data without any filter or running mean. The Spearman rank correlation coefficient was used to analyze the significance of trends due to its robustness to deviations from linearity and its resistance to the influence of outliers.

2.6. Control of thermohaline changes

Temperature variability along the water column will be interpreted using the model proposed by Bindoff and McDougall, (1994). According to their methodology it is possible to know if changes in a scalar property detected along isobars are due to changes on isopycnals or vertical displacements of isopycnals. Changes on isopycnals are related to heat flux variability (pure warming) and freshwater flux variability (pure freshening) in the water formation area (Jackett and McDougall, 1997; Arbic and Owens, 2001). On the other hand, vertical displacements of isopycnals are related to the process that Bindoff and McDougall, (1994) define as pure heaving. This process results in water masses sinking or rising without changing their intrinsic properties. These displacements are caused by wind stress variability or changes in the water

formation rates. The model proposed by Bindoff and McDougall, (1994) is applied following

$$\left.\frac{d\varepsilon}{dt}\right|_p = \left.\frac{d\varepsilon}{dt}\right|_n - \left.\frac{dp}{dt}\right|_n \left(\frac{\delta\varepsilon}{\delta p}\right) \quad (5)$$

where $|_p$ denotes changes along pressure surfaces and $|_n$ accounts for changes along neutral surfaces. The left term ($\left.\frac{d\varepsilon}{dt}\right|_p$) accounts for time variation of a scalar property (potential temperature in the present study) along isobars. The first term on the right hand ($\left.\frac{d\varepsilon}{dt}\right|_n$) accounts for time variation of the scalar property along isopycnals. The last term ($\left.\frac{dp}{dt}\right|_n \left(\frac{\delta\varepsilon}{\delta p}\right)$) takes into account the rate of change of isopycnals displacements ($\left.\frac{dp}{dt}\right|_n$) and the vertical gradient of the scalar property ($\frac{\delta\varepsilon}{\delta p}$), which together refer to the vertical displacement of isopycnals. Vertical gradients are assumed to be constant in time.

3. Results and discussion

The SST climatology calculated at monthly scale over the period 1982-2015 is shown in Figure 2. Overall, two different patterns are observed in the area throughout the year. On the one hand, from November to April similar values are detected between coastal and oceanic locations on the Yucatan shelf (around 23.5-26ºC depending on the month). Moreover, a tongue of warmer water (values around 26-27.5ºC) spreads from the Caribbean Sea through the Yucatan Channel during these months. Colder water is observed from June to September near the northern coast of Yucatan in contrast with the warmer oceanic water, the difference between both water masses is close to 2.5ºC.

Finally, May and October can be considered as transition months since cold water is observed in the shelf of North Yucatan although the differences between coast and ocean are small. Seasonal SST differences between coast and ocean had been also observed in some of the most important upwelling systems in the world as Benguela, Canary, La Guajira or Java (Lemos and Sansó, 2006, Santos et al., 2012a,b,c, Santos et al., 2016, Varela et al., 2016). In the case of North Yucatan, SST differences between coast and ocean can be related to the existence of a relatively strong upwelling in the area (Pérez-Santos et al., 2010, Ruiz–Castillo et al., 2016). Mendoza et al., (2005) used a model based in the thermal energy equation to simulate SST in the Gulf of Mexico obtaining differences around 3ºC in July between coast and the adjacent ocean zone. Similar results were obtained by Zavala-Hidalgo et al., (2006) who observed colder coastal water north of Yucatan Peninsula from May to August with a peak in July.

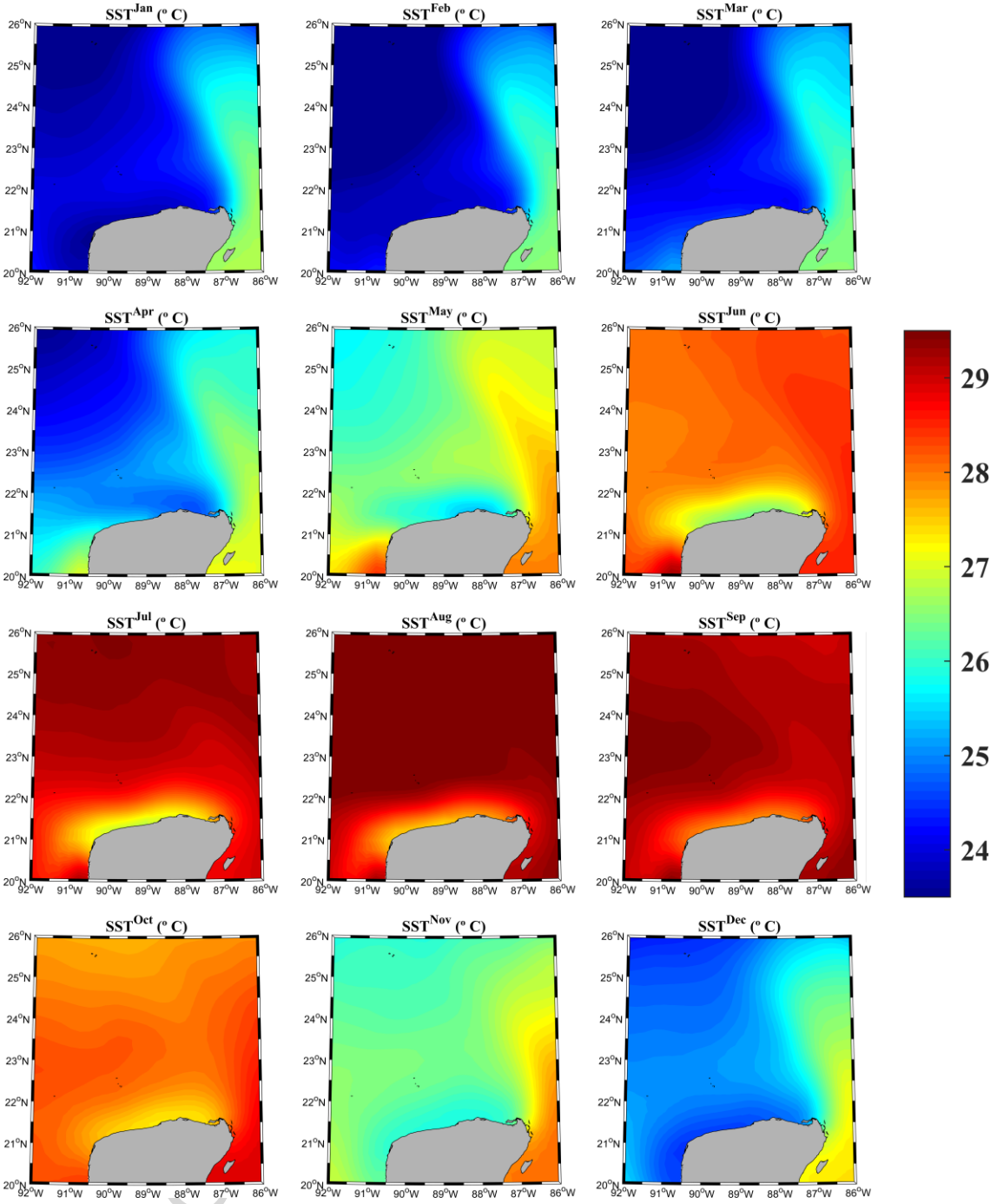

Figure 2 | Monthly mean SST (ºC) over the period 1982-2015 obtained from OISST$^{1/4}$ database.

Differences between coastal and oceanic locations are represented in Figure 3. Points where SST was averaged to obtain coastal (black dots) and oceanic (black crosses) values are marked in Figure 1. Blue (red) line identifies the annual cycle of SST for

coastal (oceanic) locations averaged meridionally. Oceanic SST shows higher values when compared with coastal locations. The lowest ocean temperatures are found from January to March (24ºC) and the highest ones in August (up to 29.5ºC). Similar results are observed near coast but the highest SST value was found in September (28ºC). Although ocean SST is always higher than near coast, the greatest differences are found from May to September, ranging from around 1ºC in May to near 2ºC in August. Reyes-Mendoza et al., (2016), who analyzed the effects of wind on upwelling off Cabo Catoche, detected that upwelling was higher from March to September. These results are consistent with those obtained in Figure 2 and allow focusing the present study on May-September months, when the highest differences between coastal and oceanic SST were found.

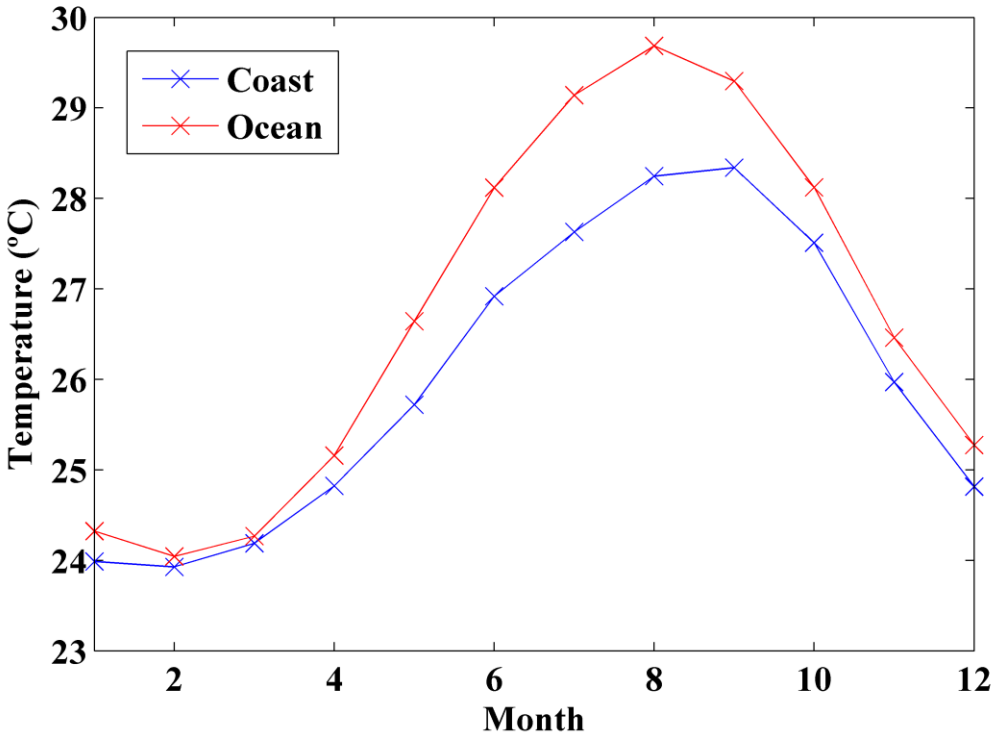

Figure 3 | Annual cycle of SST (°C) meridionally averaged at coastal (blue line) and ocean locations (red line) over the period 1982 to 2015 using OISST$^{1/4}$ database. Sampling points marked in Figure 1.

Figure 4a shows SST trends over the period May to September, when the difference between coast and ocean is more visible. An increasing pattern is obtained for ocean locations with values ranging from 0.1 to 0.2ºC dec^{-1}. A negative trend was observed at coastal locations (-0.1ºC dec^{-1}). Thus, the difference between coastal and oceanic rates is higher than 0.25ºC dec^{-1}. This behavior had also been observed in some of the major upwelling systems in the world. Santos et al., (2012b) found different rates between coast and ocean higher than 0.3ºC dec^{-1} in the Benguela Upwelling System from 1970 to 2009. In the case of Canary Upwelling System, Santos et al., (2012c) observed differences up to 0.1ºC dec^{-1} from 1982 to 2010. For the cases of Java or La Guajira, Varela et al., (2016) and Santos et al., (2016) found different rates between coast and ocean around 0.3ºC dec^{-1} respectively over the last three decades. A complete study of worldwide SST trends can be observed in Cheung et al., (2013). Figure 4b shows the temporal variability of SST corresponding to the upwelling season (May-September) from 1982 to 2015 both near coast and at the ocean. In general, coastal points (blue) show lower temperatures than the oceanic points (red). Being the coastal trend negative (cooling) and the oceanic one positive (warming), the difference between both signals tends to increase in time, especially since 2000. These results are in good agreement with the pattern shown in Figure 4a.

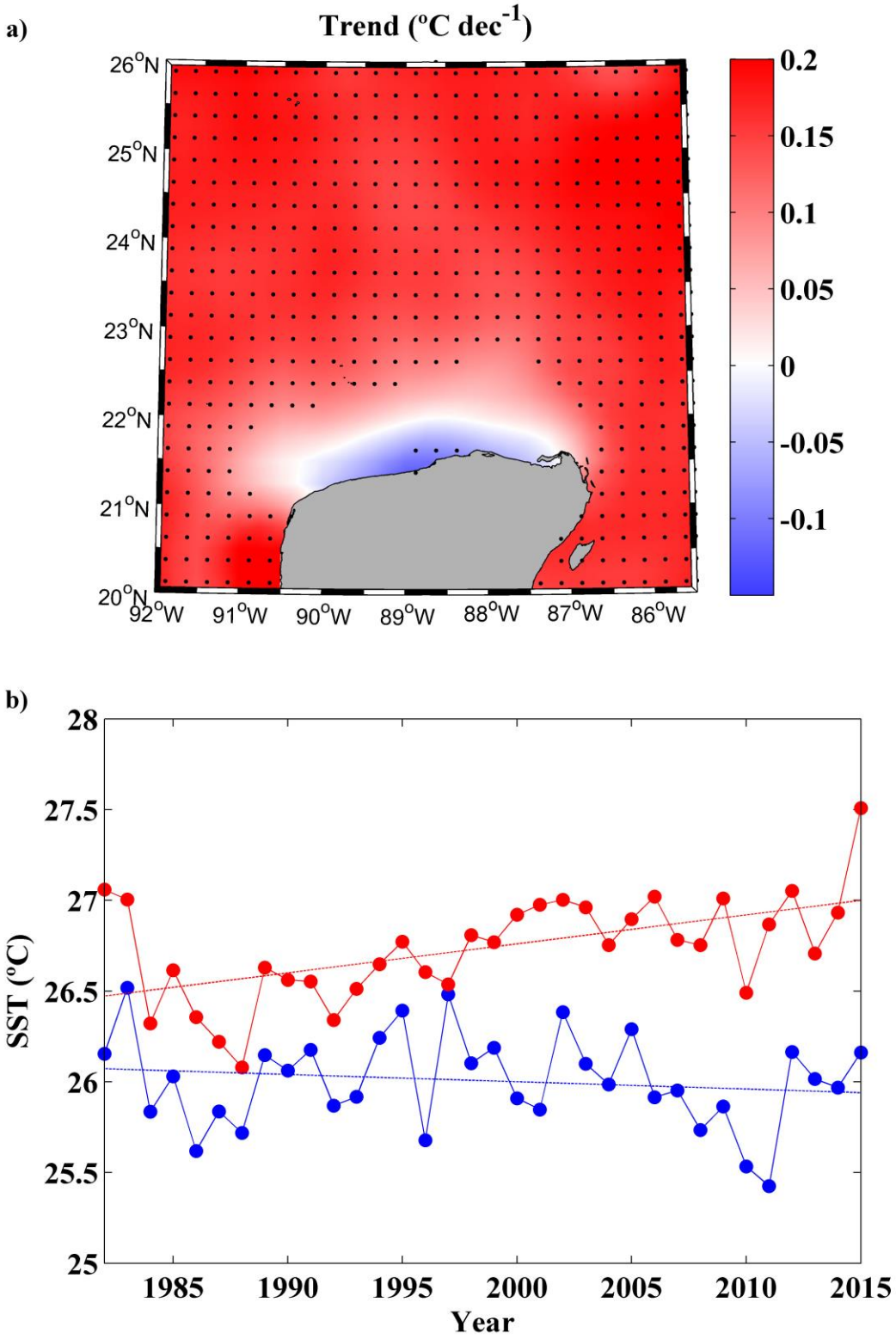

Figure 4 | (a) May-September SST trend (°C dec^{-1}) calculated over the period 1982-2015 using OISST$^{1/4}$ database. **(b) Temporal variability of SST (ºC)** at coastal (blue line) and ocean locations (red line) over the period 1982 to 2015 from May to September at the points marked in Figure 1 (dots and crosses).

Overall, the presence of cooling trends has been associated to the reinforcement of upwelling in some areas (Benguela, Canary, Peru) (Narayan et al., 2010, Patti et al., 2010, Rahn and Garreaud, 2013, Cropper et al., 2014). However, this behaviour has not been homogeneous among the worldwide upwelling systems showing, in some cases, a weakening in upwelling (Varela et al., 2015). To analyze the possible causes of these different warming rates, the upwelling index trend was calculated over the period 1982-2015 considering the spring-summer seasons (May-September) (Figure 5). Negative upwelling trends were obtained for the whole area with values between -0.055 m^2 s^{-1} dec^{-1} and -0.090 m^2 s^{-1} dec^{-1}. Thus, it is evident that the reinforcement of upwelling in the area is not the main factor that drives cooling SST trends in the Northern coast of Yucatan.

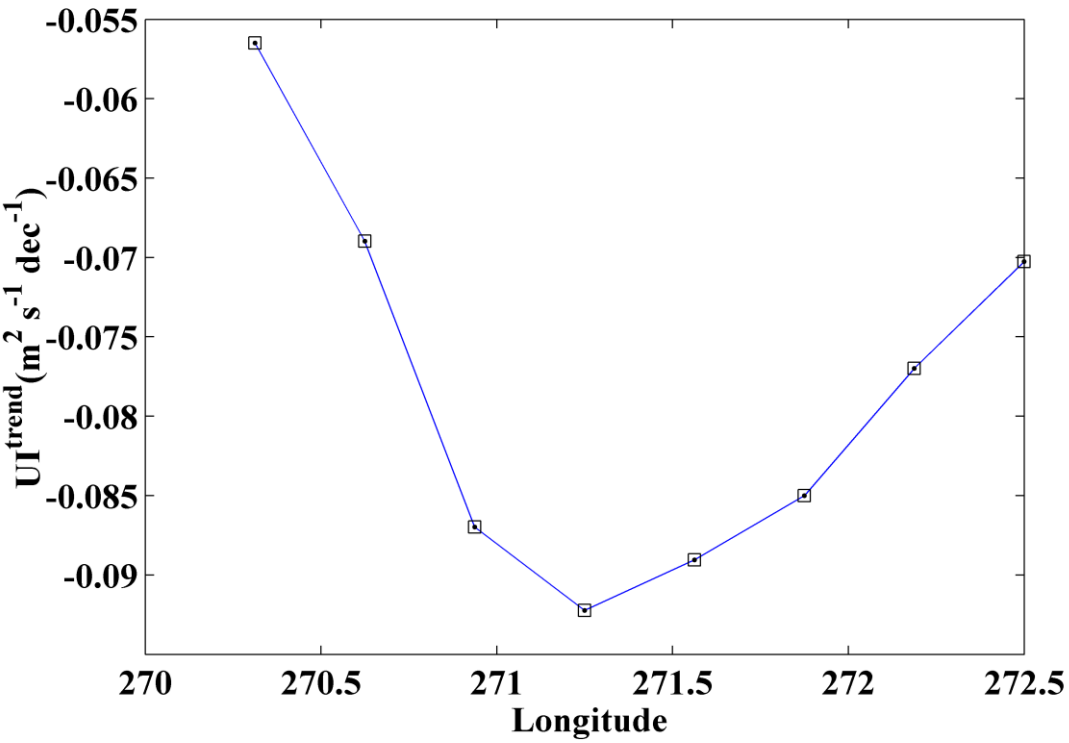

Figure 5 | UI trend (m^2 s^{-1} dec^{-1}) calculated over the period 1982 to 2015 averaged from May to September using CFSR database.

Once changes in upwelling have been dismissed as a driver in coastal cooling, variations in the total heat flux between atmosphere and sea were also calculated (Figure 6). Total heat flux trends show an increase for most of the area with values between 6–12 W m^{-2} dec^{-1}, which means that ocean has gained heat during the last decades. Coastal and oceanic locations did not show any difference in heat exchange variability in the upwelling area so, heat exchange between atmosphere and ocean, should also be discarded as a key factor in the occurrence of near shore cooling.

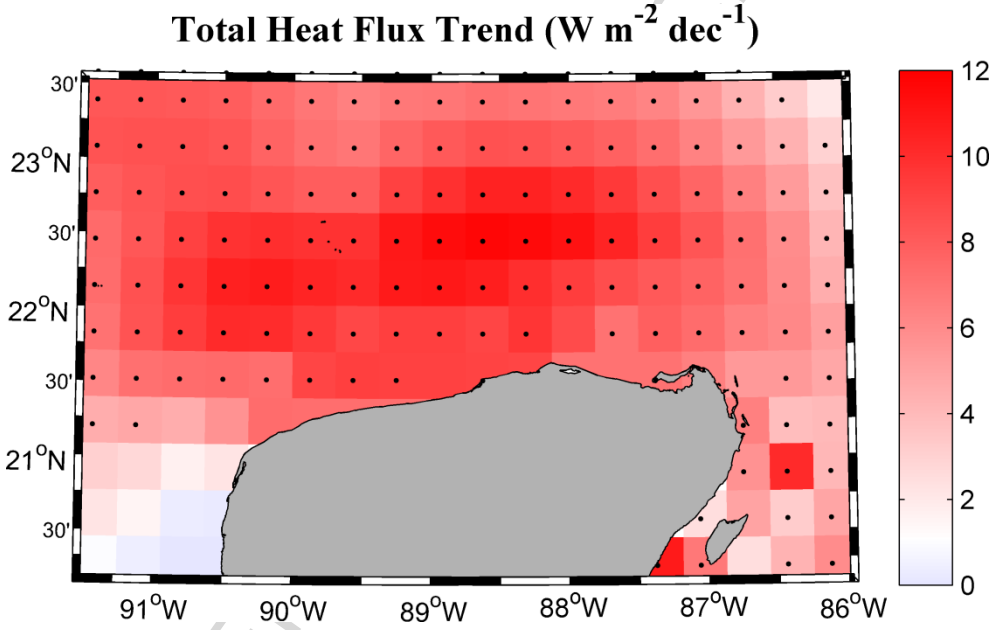

Figure 6 | Heat flux trend (W m^{-2} dec^{-1}) calculated over the period 1982–2015 (May-September). Black dots represent grid points with significance higher than 95%. A negative (positive) value implies that ocean is losing (gaining) heat.

As previously mentioned, the Yucatan Current can be one of the factors responsible of the SST variability detected along the North Yucatan coast because it conditions upwelling processes that bring water from the Caribbean Sea to the Yucatan Shelf (Merino, 1997; Zavala-Hidalgo et al., 2006; Carrillo et al., 2016; Souza et al., 2016).

Different mechanisms have been suggested to explain the relation between the upwelled water and the YC. Cochrane, (1963; 1966) proposed that friction from the bottom layer with the YC generates a vertical Ekman transport, while Bulanienkov and García, (1973) suggested that the interaction between the YC and the undercurrent off Cuba originated the vertical transport. More recently, Enríquez and Mariño-Tapia, (2014) observed that the trajectory of the YC is important in the development of upwelling. Using a numerical model they proved that, when the YC is directed to the northeast, vertical velocities became positive along the continental slope favoring the appearance of colder water over the Yucatan Shelf. Thus, a northeast trajectory of the YC can lead to changes in the thermohaline properties of the sea water that extends towards the west along the Yucatan Shelf. In addition, Carrillo et al., (2016) observed through in-situ data collected in oceanographic cruises, that upwelling was stronger in the area north of 21ºN when the YC separates from the coast. A similar phenomenon was previously described in the Agulhas Bank to explain upwelling (Lutjeharms et al., 2000). Souza et al., (2016) also hypothesized that the interaction between YC and topography could explain upwelling.

Therefore, it is crucial to analyze YC variability to know whether or not cooling along the north coast of Yucatan Peninsula can be related to changes in the YC trajectory. With this aim the following procedure was applied: a) The YC path along the eastern area of the Yucatan Peninsula was defined as the vein of maximum current velocity in the sub-surface. An average between 100m and 150m depth was considered following previous studies (Hernández-Guerra and Joyce, 2000; Enríquez et al., 2013; Carrillo et al., 2016); b) the pixel with the maximum module velocity was selected for each latitude and for each month. Thus, for example, to detect where the core was at 20.25ºN at a certain month all pixels corresponding to this latitude between 84-87ºW were

analyzed and the pixel with the maximum module velocity was considered as the location where the core of the YC flows at this particular month. A value of 1 was assigned to the selected pixel and 0 to the rest. This procedure was repeated for each latitude (from 20.25ºN to 23 ºN) and for each month, considering only May-September months from 1993 to 2015. In this way, the summation of all images corresponding to each month show the most usual path (Figure 7a). Results are represented as the percentage of times that the maximum velocity was detected. Thus, a value of 70 means that the maximum current velocity at a particular latitude was found, at that pixel, 70% of the months. Figure 7a represents the most usual path where the YC core flows. This stream flows between 86º-87º W following the continental slope among 20-22º N (Figure 1). c) Once the path of the YC core was detected for each month, two periods (1993-2003 and 2005-2015) were compared to detect possible changes in the YC path. A composite of images was built for every period and the composite of the first period was subtracted from the one of the last period. Changes in the YC direction from 1993 to 2015 are shown in Figure 7b. Negative values (blue) denote the prevalent path during the first decade, while positive values (red) show the prevalent path during the last decade. Therefore, it was observed that YC has shifted to the east at 21-22º N. According to Enríquez and Mariño-Tapia, (2014), this shift should favor a greater vertical transport along the continental slope, which in turn, would cause thermohaline variations in the upwelled sea water. To confirm this fact, temperature variability was analyzed along the transect shown in Figure 1 (black solid line), which was selected following the procedure described above (see Figure 7a).

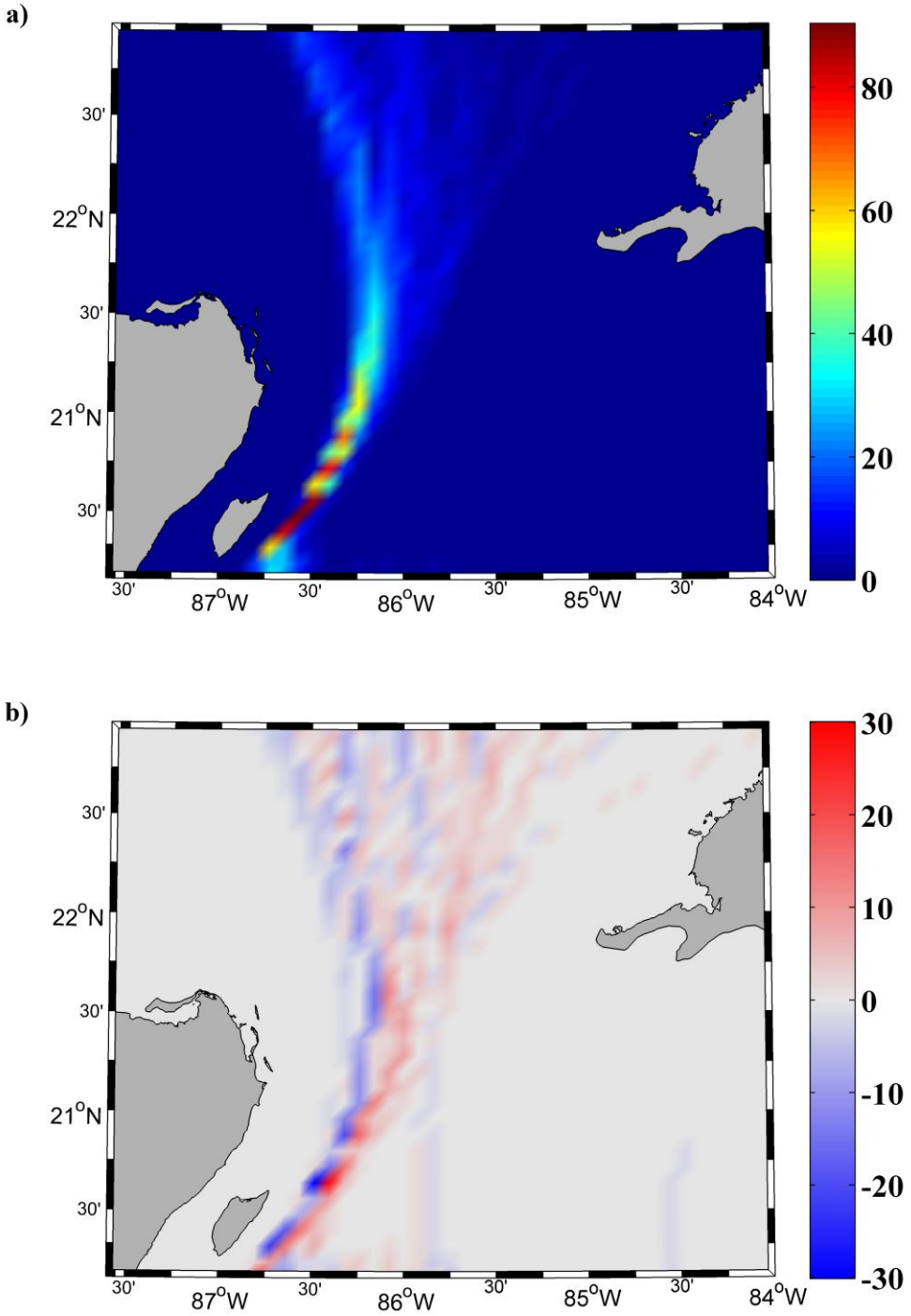

Figure 7 | (a) Path followed by the Yucatan Current core averaged over the period 1993-2015 considering May-September months. **(b) Evolution of the Yucatan Current path** from 1993 to 2015 (May-September) using HYCOM database. Negative values (blue) denote the path of the YC in the first decade (1993-2003) and positive values (red) denote the path of the YC in the last decade (2005-2015).

Thus, temperature trends for the upper 400m of the water column along that transect are represented in Figure 8 over the period 1993-2015 (May-September). The most remarkable feature is that cooling (~-0.3ºC dec^{-1}) was observed between 50-200m only at the northern part of the studied transect. That area coincides with the location where the Caribbean Subtropical Underwater (CSUW) water mass upwells to the Yucatan shelf (Enríquez et al., 2013; Ramos-Musalem, 2013; Carrillo et al., 2016). This water mass has its core around 100-150m deep (Hernández-Guerra and Joyce, 2000; Enríquez et al., 2013; Carrillo et al., 2016).

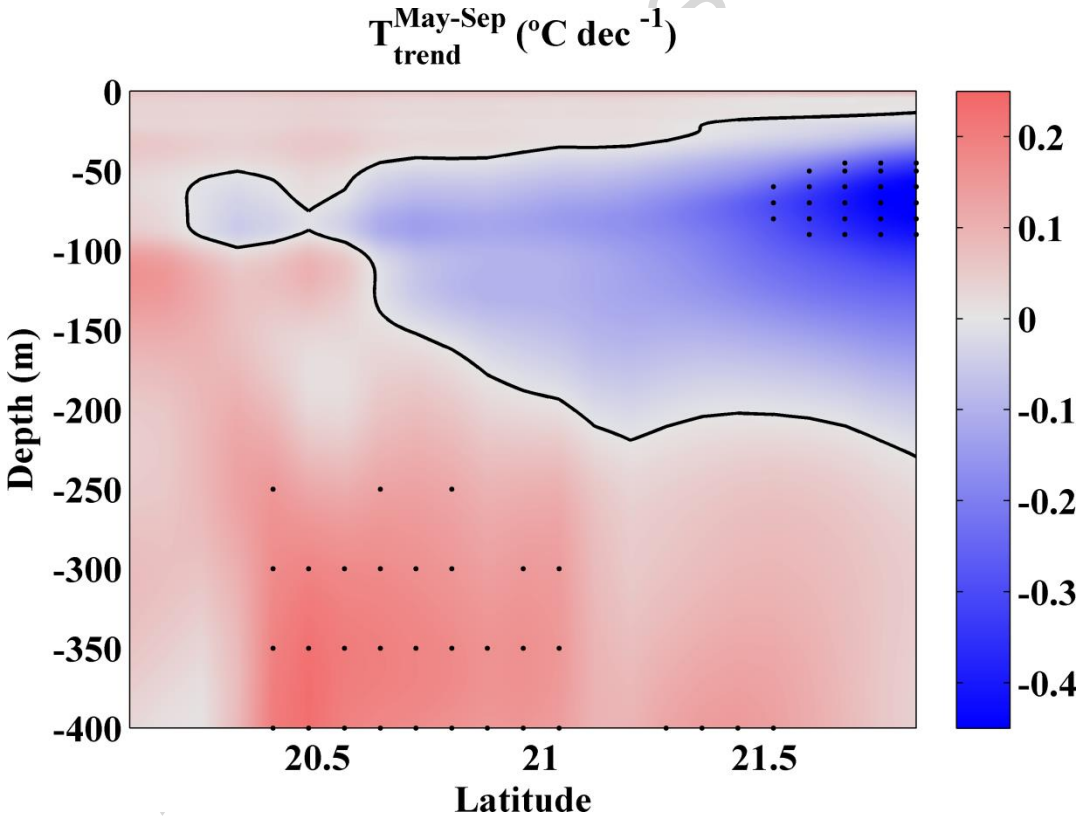

Figure 8 | Temperature trend (°C dec^{-1}) calculated using HYCOM database over the period 1993-2015 for May-September months at the upper 400m of the water column (solid line in Figure 1). The contour line corresponds to the absence of trend. Black dots represented those points with a significance higher than 90%.

In order to analyze the thermal variability along the water column in the area where the water from the Yucatan current uploads the Yucatan shelf, different transects (green lines in Figure 1) were defined along the eastern area of the Yucatan Shelf. Figure 9 shows the temperature trends from May to September at four different transects. Overall, cooling trends can be observed along the path followed by the Yucatan Current, from near surface up to 400 meters. This cooling is significant at around 150 meters depth, which corresponds to the core of the current. Further west, it can be seen clearly (a contour corresponding with neutral trends was depicted to facilitate its visualization) how cool water upwells to the Yucatan shelf. However, it is important to note that cooling only reaches the sea surface at latitudes from 21.75 ºN (Figure 9b) and 22ºN (Figure 9c), while north and south of this section (Figure 9a and 9d) cooling does not reach the sea surface.

Therefore, it can be concluded that the sea water that upwells from the Caribbean Sea and expands along the deepest layers of the Yucatan shelf has cooled over the period 1993-2015. It results from the uplifting of cold water from depths around 150m to the surface at a latitude ranging from 21.75ºN to 22ºN. This fact explains the contrast between cooling along the coast and warming in the oceanic area of the Yucatan shelf (Figure 4a). The cold water that upwells at the Yucatan shelf occupies the bottom layers (Enríquez et al., 2013) and it only appears near surface at a narrow fringe near coast due to the upwelling caused by the prevalence of trade winds in the region. For this reason, cooling does not appear north of 22º N.

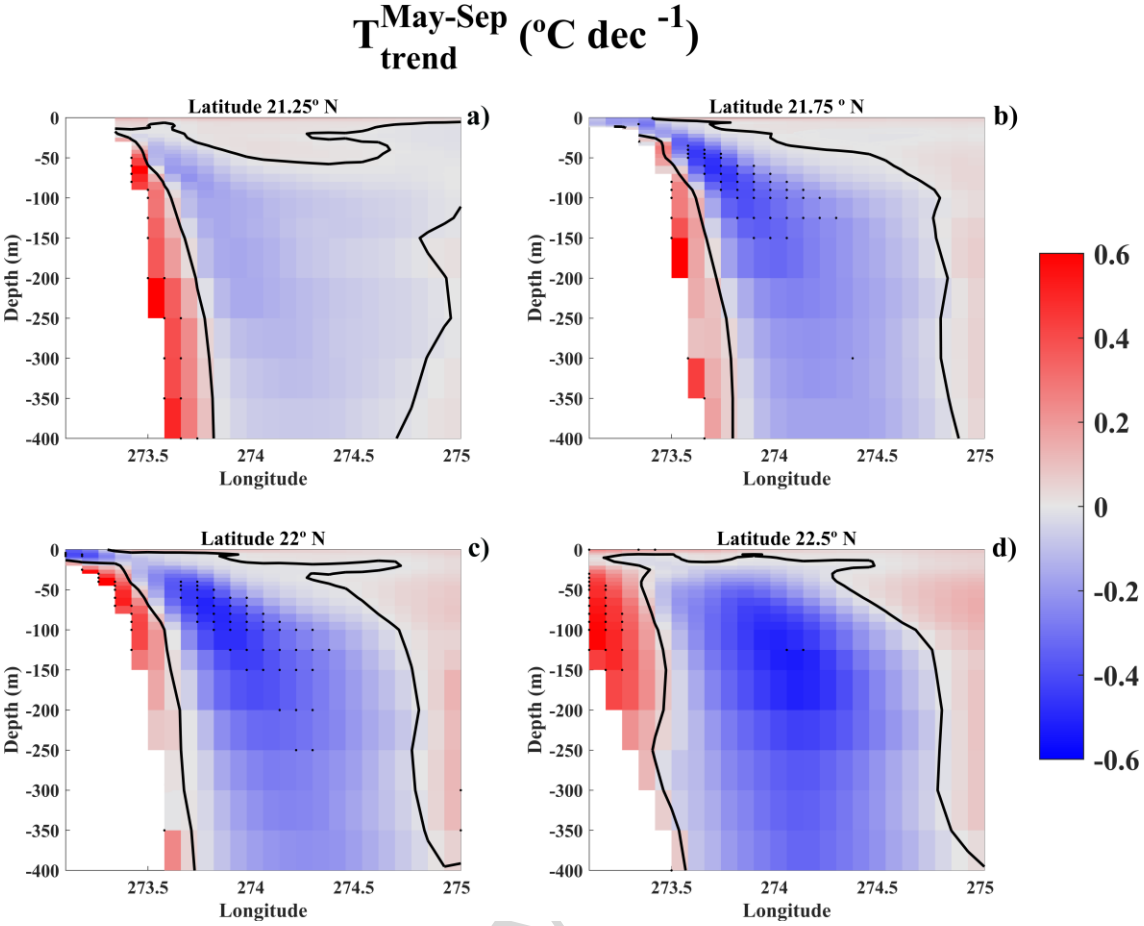

Figure 9 | Temperature trend (°C dec^{-1}) calculated using HYCOM database over the period 1993-2015 during the upwelling season (May-September) at four transects depicted in Figure 1 (green lines). The contour line corresponds to the absence of trend. Black dots represented those points with a significance higher than 90%.

Finally, the model proposed by Bindoff and McDougall, (1994) (see eq. (5)) was applied to analyze the cause of the changes detected in Figure 8. The model was applied to the northern half of the transect (north of 21°N) since it is the area where significant cooling was observed. According to Figure 10, cooling was detected along isobars (red line) from 50m to 150m, in good agreement with Figure 8, with a maximum cooling rate (~-0.02°C y^{-1}) at ~75m. It can be observed that cooling is mainly due to vertical displacement of isopycnals (green line) in the upper part of the water column (50-

100m), although a slight cooling was detected from 100m to 150m mainly due to changes in the intrinsic properties of the water (red line). Taking into account that temperature decreases with increasing depth, it can be concluded that the observed cooling was caused by the uplifting of isopycnals. This fact is consistent with previous research. Merino, (1997) observed the raise of isotherms and isohalines in the area. Ramos-Musalem, (2013) also found water uplift from 120m until less than 40m along the eastern part of the Yucatan Shelf.

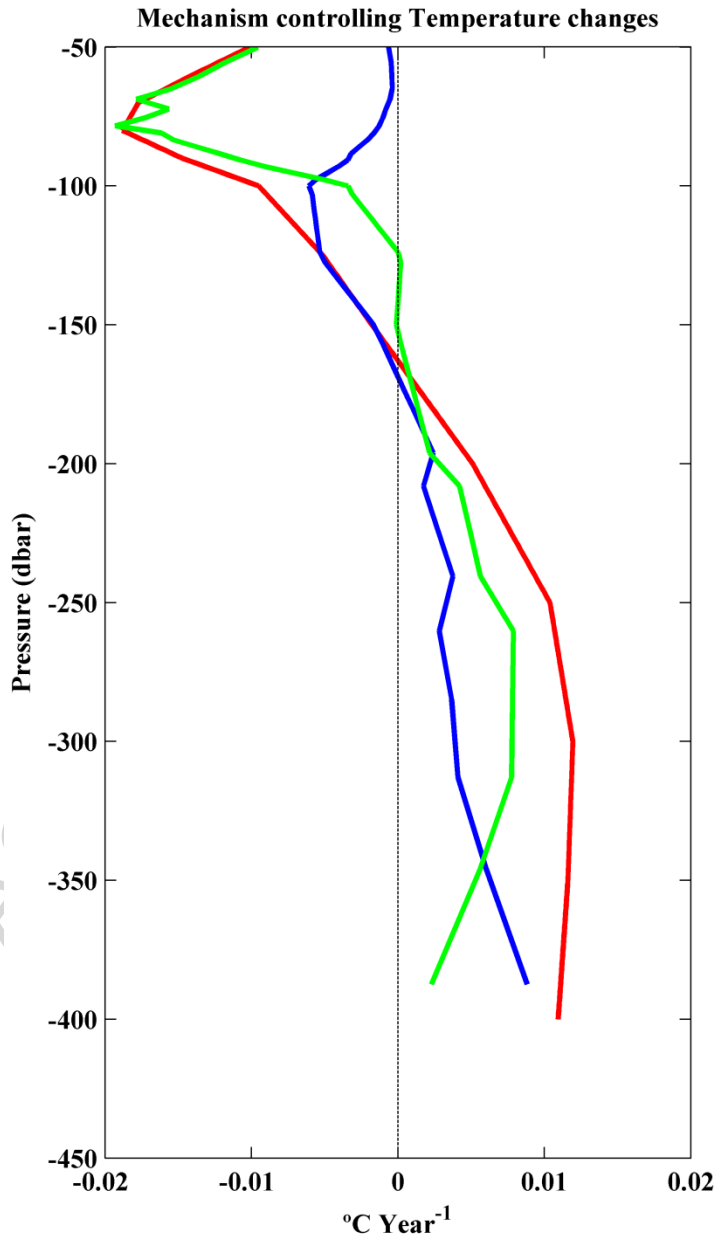

Figure 10 | Decomposition of temperature changes along isobars (red line) as the sum of changes along isopycnals (blue line) and changes due to vertical displacement of isopycnals (green line).

4. Summary

Sea surface warming was detected at oceanic locations north of Yucatan Peninsula and cooling was observed at the coastal zone, especially over the period May-September. Whilst the amplitude of ocean warming is similar to the amplitude found in most of the North Atlantic areas, coastal cooling constitutes a differential fact.

Analyzing near-shore thermal variability at the Yucatan shelf is a complex task since the area is under the influence of different drivers. Despite wind induced upwelling plays a key role in the area, the observed decrease in upwelling index is not consistent with coastal cooling. In a similar way, the sea-atmosphere heat exchange is homogeneous for the whole area, without differences between coast and ocean. Consequently, heat exchange should also be discarded as a possible reason for near-shore cooling.

On the other hand, previous authors suggested that the Yucatan Current could have an important role in the spread of the upwelling. The analysis of the path of the Yucatan Current showed a shift to the east which favors an enhancement of the vertical transport in the eastern part of the Yucatan Shelf. Moreover, cooling can be observed along the path followed by the Yucatan Current (approximately at a deep of 150m), which upwells to the surface at 21.75ºN-22ºN near Cabo Catoche (Figure 9) due to the uplifting of isopycnals (Figure 10). This cold water occupies the deepest layers over the continental shelf and is pumped by upwelling caused by favorable westerly winds, which makes the cold signal visible at sea surface near shore.

Acknowledgment

This work was partially supported by Xunta de Galicia under Project ED431C 2017/64-GRC "Programa de Consolidación e Estruturación de Unidades de Investigación Competitivas (Grupos de Referencia Competitiva)". R. Varela is supported by the University of Vigo through the *Axudas predoutorais da convocatoria de axudas a investigación 2015*. X. Costoya is supported by the Portuguese Science Foundation (FCT) through a Post-doctoral grant (SFRH/BPD/118142/2016). CFSR data was obtained from Environmental Modeling Center/National Centers for Environmental Prediction/National Weather Service/NOAA/U.S. NCEP Climate Forecast System Reanalysis (CFSR) Monthly Products. Research Data Archive at the National Center for Atmospheric Research, Computational and Information Systems Laboratory. http://rda.ucar.edu/datasets/ds093.2/. Funding for the development of HYCOM has been provided by the National Ocean Partnership Program and the Office of Naval Research. Data assimilative products using HYCOM are funded by the U.S. Navy. Computer time was made available by the DoD High Performance Computing Modernization Program. The output is publicly available at http://hycom.org.

References

1- Levitus, S., Antonov, J. and Boyer, T. Warming of the world ocean, 1955–2003. Geophysical Research Letters, 2005, 32(2). DOI: 10.1126/science.287.5461.2225.

2- Mikaloff-Fletcher, S. E., Gruber, N., Jacobson, A. R., Doney, S. C., Dutkiewicz, S., Gerber, M., Follows, M., Joos, F., Lindsay, K., Menemenlis, D., Mouchet, A., Muller, S. A. and Sarmiento, J. L. Inverse estimates of anthropogenic CO2 uptake, transport, and storage by the ocean. Global Biogeochemical Cycles, 2006, 20(2). DOI: 10.1029/2005GB002530.

3- Levitus, S., Antonov, J. I., Boyer, T. P., Baranova, O. K., Garcia, H. E., Locarnini, R. A., Mishonov, A. V., Reagan, J. R., Seidov, D., Yarosh, E. S. and Zweng, M. M. World ocean heat content and thermosteric sea level change (0–2000 m), 1955–2010. Geophysical Research Letters, 2012, 39(10). DOI: 10.1029/2012GL051106.

4- Pauly, D. and Christensen, V. Primary production required to sustain global fisheries. Nature, 1995, 374(6519), 255. DOI: 10.1038/376279b0.

5- Harrison, D. E. and Carson, M. Is the world ocean warming? Upper ocean trends, 1950–2000. Journal of Physical Oceanography; 2007, 37: 174–187. https://doi.org/10.1175/JPO3005.1

6- Lima, F. P. and Wethey, D. S. Three decades of high-resolution coastal sea surface temperatures reveal more than warming. Nature Communications; 2012, 3: 704. DOI:10.1038/ncomms1713.

7- Cheung, W. W. L., Watson, R. and Pauly, D. Signature of ocean warming in global fisheries catch, *Nature*, 2013, 497, 365- 369. DOI:10.1038/nature12156.

8- Lemos, R. T. and Sansó, B. Spatio-temporal variability of ocean temperature in the Portugal Current System. Journal of Geophysical Research; 2006, 111: C04010. DOI: 10.1029/2005JC003051.

9- Santos, F., Gómez-Gesteira, M., deCastro, M. and Álvarez, I. Variability of coastal and ocean water temperature in the upper 700 m along the Western Iberian Peninsula from 1975 to 2006. PLoS One; 2012a, 7(12): 1–7. https://doi.org/10.1371/journal.pone.0050666

10- Santos, F., Gómez-Gesteira, M., deCastro, M. and Álvarez, I. Differences in coastal and oceanic SST trends due to the strengthening of coastal upwelling along the Benguela current system. Continental Shelf Research; 2012b, 34: 79–86. https://doi.org/10.1016/j.csr.2011.12.004

11- Santos, F., Gómez-Gesteira, M., deCastro, M. and Álvarez, I. Differences in coastal and oceanic SST warming rates along the Canary Upwelling Ecosystem from 1982 to 2010. Continental Shelf Research; 2012c, 47: 1–6. https://doi.org/10.1016/j.csr.2012.07.023

12- Santos, F., Gómez-Gesteira, M., Varela, R., Ruiz-Ochoa, M. and Días, J. M Influence of upwelling on SST trends in La Guajira system. Journal of Geophysical Research: Oceans, 2016, 121(4), 2469-2480. DOI: 10.1002/2015JC011420

13- Varela, R., Santos, F., Gómez-Gesteira, M., Álvarez, I., Costoya, X. and Días, J. M. Influence of Coastal Upwelling on SST Trends along the South Coast of Java. PloS one, 2016, 11(9), e0162122. https://doi.org/10.1371/journal.pone.0162122

14- Varela, R., Álvarez, I., Santos, F., deCastro, M. and Gómez-Gesteira, M. Has upwelling strengthened along worldwide coasts over 1982-2010? Scientific reports, 2015, 5. DOI:10.1038/srep10016

15- Ruiz-Castillo, E., Gomez-Valdes, J., Sheinbaum, J. and Rioja-Nieto, R. Wind-driven coastal upwelling and westward circulation in the Yucatan shelf. Continental Shelf Research, 2016, 118, 63-76. https://doi.org/10.1016/j.csr.2016.02.010

16- Merino, M. Upwelling on the Yucatan Shelf: hydrographic evidence. Journal of Marine Systems, 1997, 13(1-4), 101-121. https://doi.org/10.1016/S0924-7963(96)00123-6

17- Pérez-Santos, I., Schneider, W., Sobarzo, M., Montoya-Sánchez, R., Valle-Levinson, A. and Garcés-Vargas, J. Surface wind variability and its implications for the Yucatan Basin-Caribbean Sea dynamics. Journal of Geophysical Research, 2010, 115. DOI: 10.1029/2010JC006292

18- Enríquez, C., Marino-Tapias, I., Jerónimo, G. and Capurro-Filograsso, L. Thermohaline processes in a tropical coastal zone. Continental Shelf Research, 2013, 69, 101-109. https://doi.org/10.1016/j.csr.2013.08.018

19- Salmerón-García, O., Zavala-Hidalgo, J., Mateos-Jasso, A. and Romero-Centeno, R. Regionalization of the Gulf of Mexico from space-time chlorophyll-a concentration variability. Ocean Dynamics, 2011, 61(4), 439-448. https://doi.org/10.1007/s10236-010-0368-1

20- Pérez-Santos, I., Schneider, W., Valle-Levinson, A., Garces-Vargas, J., Soto, I., Montoya-Sanchez, R. and Müller-Karger, F. Chlorophyll-a patterns and mixing processes in the Yucatan Basin, Caribbean Sea. Patrones superficiales de la clorofila a y procesos de mezcla en la cuenca de Yucatán, mar Caribe. Ciencias Marinas, 2014, 40(1), 11-31. http://dx.doi.org/10.7773/cm.v40i1.2320

21- Cárdenas-Palomo, N., Herrera-Silveira, J., Velázquez-Abunader, I., Reyes-Mendoza, O. and Ordoñez, U. Distribution and feeding habitat characterization of whale sharks *Rhincodon typus* in a protected area in the north Caribbean Sea. Journal of Fish Biology, 2015, 86(2), 668-686. DOI: 10.1111/jfb.12589

22- Zavala-Hidalgo, J., Gallegos-García, A., Martínez-López, B., Morey, S. L and O'Brien, J. J. Seasonal upwelling on the western and southern shelves of the Gulf of Mexico. Ocean Dynamics, 2006, 56(3-4), 333-338. https://doi.org/10.1007/s10236-006-0072-3

23- del Monte-Luna, P., Villalobos, H. and Arreguín-Sánchez, F. Variability of sea surface temperature in the southwestern Gulf of Mexico. Continental Shelf Research, 2015, 102, 73-79. https://doi.org/10.1016/j.csr.2015.04.017

24- Enríquez, C. and Mariño-Tapias, I. Mechanisms driving a coastal dynamic upwelling. In Proceedings of the 17th Physics of Estuaries and Coastal Seas (PECS) Conference. 2014.

25- Reyes-Mendoza, O., Mariño-Tapias, I., Herrera-Silveira, J., Ruiz-Martínez, G., Enríquez, C. and Largier, J. L. The effects of wind on upwelling off Cabo Catoche. Journal of Coastal Research, 2016, 32(3), 638–650. https://doi.org/10.2112/JCOASTRES-D-15-00043.1

26- Souza, A. J., Mariño-Tapias, I. and J-M Hirschi, J. Mechanisms controlling upwelling on the Yucatan shelf; its interannual variability and predictability. In Abstract for the 18th Physics of Estuaries and Coastal Seas Conference. 2016.

27- Carrillo, L., Johns, E. M., Smith, R. H., Lamkin, J. T. and Largier, J. L. Pathways and hydrography in the Mesoamerican Barrier Reef System Part 2: Water masses and thermohaline structure. Continental Shelf Research, 2016, 120, 41-58. https://doi.org/10.1016/j.csr.2016.03.014

28- Reynolds, R. W. What's new in Version 2 [Available at http//www.ncdc.noaa.gov/oa/climate/research/sst/papers/whats_new_v2.pdf.] 2009.

29- Reynolds, R. W. and Chelton, D. W. Comparisons of daily sea surface temperature analysis for 2007–08. Journal of Climate; 2010, 23: 3545–3562. https://doi.org/10.1175/2010JCLI3294.1

30- Cummings, J. A. Operational multivariate ocean data assimilation. Quarterly Journal of the Royal Meteorological Society Part C., 2005, 131(613):3583-3604. DOI: 10.1256/qj.05.105

31- Cummings, J. A. and Smedstad, O. M. Variational Data Assimilation for the Global Ocean. Data Assimilation for Atmospheric, Oceanic and Hidrologic Aplications vol. II, chapter 13, 2013, 303-343. https://doi.org/10.1007/978-3-642-35088-7_13

32- Saha, S., Moorthi, S., Pan, H., Wu, X., Wang, J., Nadiga, S., Tripp, P., Kistler, R., Woollen, J., Behringer, D., Liu, H., Stokes, D., Grumbine, R., Gayno, G., Wang, J., Hou, Y., Chuang, H., Juang, H. H., Sela, J., Iredell, M., Treadon, R., Kleist, D., Van Delst, P., Keyser, D., Derber, J., Ek, M., Meng, J., Wei, H., Yang, R., Lord, S., Van Den Dool, H., Kumar, A., Wang, W.,Long, C., Chelliah, M., Xue, Y., Huang, B., Schemm, J., Ebisuzaki, W., Lin, R., Xie, P., Chen, M., Zhou, S., Higgins, W., Zou, C., Liu, Q., Chen, Y., Han, Y., Cucurull, L., Reynolds, R. W., Rutledge, G. and Goldberg, M. The NCEP Climate Forecast System Reanalysis. Bulletin of the American Meteorology Society, 2010, 91: 1015–1057. https://doi.org/10.1175/2010BAMS3001.1

33- Nykjaer, L. and Van Camp, L. Seasonal and interannual variability of coastal upwelling along northwest Africa and Portugal from 1981 to 1991. Journal of Geophysical Research; 1994, 99: 14,197–14,207. DOI: 10.1029/94JC00814

34- Bindoff, N. L. and McDougall, T. J. Diagnosing climate change and ocean ventilation using hydrographic data. Journal of Physical Oceanography, 1994, 24, 1137–1152. https://doi.org/10.1175/1520-0485(1994)024<1137:DCCAOV>2.0.CO;2

35- Jackett, D. R. and McDougall, T. J. A neutral density variable for the world's oceans. Journal of Physical Oceanography, 1997, 27, 237–263. https://doi.org/10.1175/1520-0485(1997)027<0237:ANDVFT>2.0.CO;2

36- Arbic, B. K. and Owens, W. B. Climatic warming of the Atlantic intermediate waters. Journal of Climate, 2001, 14, 4091–4108. https://doi.org/10.1175/1520-0442(2001)014<4091:CWOAIW>2.0.CO;2

37- Mendoza, V. M, Villanueva, E. E. and Adem, J. On the annual cycle of the sea surface temperature and the mixed layer depth in the Gulf of México. Atmósfera, 2005, 18(2), 127-148.

38- Narayan, N., Paul, A., Mulitza, S. and Schulz, M. Trends in coastal upwelling intensity during the late 20th century. Ocean Science; 2010, 6: 815–823. DOI:10.5194/os-6-815-2010

39- Patti, B., Guisande, C., Riveiro, I., Thejll, P., Cuttitta, A., Bonanno, A., Basilone, G., Buscaino, G. and Mazzola, S. Effect of atmospheric CO 2 and solar activity on wind regime and water column stability in the major global upwelling areas. Estuarine, Coastal and Shelf Science, 2010, 88(1), 45-52. https://doi.org/10.1016/j.ecss.2010.03.004

40- Rahn, D. A. and Garreaud, R. D. A synoptic climatology of the near-surface wind along the west coast of South America. International Journal of Climatology, 2013, 34, 780-792. DOI: 10.1002/joc.3724

41- Cropper, T. E, Hanna, E. and Bigg, G. R. Spatial and temporal seasonal trends in coastal upwelling off Northwest Africa, 1981–2012. Deep-Sea Research; 2014, 1(86): 94–111. https://doi.org/10.1016/j.dsr.2014.01.007

42- Cochrane, J. D. Yucatan Current. Department of Oceanography and Meteorology, Texas A&M Univ. Ref., 1963, 63-18A, pp. 6-11

43- Cochrane, J. D. The Yucatan Current, upwelling off northeastern Yucatan, and currents and waters of western equatorial Atlantic, Oceanography of the Gulf of Mexico. Progress Reports, 1966, TAMU Ref._66-23T, pp.14–32.

44- Bulanienkov, S. K. and García, C. Influencia de los procesos atmosféricos en el afloramiento del banco de Campeche. Revista de Investigación Pesquera, 1973, 99-140.

45- Lutjeharms, J. R. E., Cooper, J. and Roberts, M. Upwelling at the inshore edge of the Agulhas Current. Continental Shelf Research, 2000, 20(7), 737-761. https://doi.org/10.1016/S0278-4343(99)00092-8

46- Hernández-Guerra, A., and Joyce, T. M. Water masses and circulation in the surface layers of the Caribbean at 66 W. Geophysical research letters, 2000, 27(21), 3497 3500.ISO 690.

47- Ramos Musalem, A. K. Estudio numérico de los forzamientos que generan la surgencia de Yucatán (Bsc. Thesis). UNAM, Mexico, 2013, p. 77**.**

Highlights

- In a context of global warming, Yucatan Shelf show cooling trends.
- Contrary to other upwelling areas, an increase of upwelling is not the main cause.
- Different drivers were assessed, highlighting the Yucatan current effects.
- A cooling in the deeper layers of the core of the Yucatan current was observed.
- Cold water over the deepest layers is pumped by upwelling favorable westerly winds.